Absorption correction: numerical (*XRED*; Stoe & Cie, 1997*a*)
T_{min} = 0.031, T_{max} = 0.233
9080 measured reflections
4196 independent reflections
R_{int} = 0.048
θ_{max} = 28.06°
$h = -11 \rightarrow 10$
$k = -11 \rightarrow 11$
$l = -18 \rightarrow 18$

Refinement

Refinement on F^2
$R[F^2 > 2\sigma(F^2)]$ = 0.032
$wR(F^2)$ = 0.044
S = 1.844
4196 reflections
144 parameters
$w = 1/[\sigma^2(F_o^2)]$
$(\Delta/\sigma)_{max}$ = 0.001
$\Delta\rho_{max}$ = 1.273 e Å^{-3}
$\Delta\rho_{min}$ = −1.865 e Å^{-3}
Extinction correction: *SHELXL*93 (Sheldrick, 1993)
Extinction coefficient: 0.00139 (11)
Scattering factors from *International Tables for Crystallography* (Vol. C)

Table 1. *Selected geometric parameters (Å, °)*

Br1—C1	1.894 (5)	C1—C6	1.374 (7)
Br2—C2	1.871 (5)	C1—C2	1.407 (7)
Br3—C3	1.908 (5)	C2—C3	1.408 (7)
Br4—C4	1.902 (5)	C3—C4	1.380 (7)
Br5—C5	1.885 (6)	C4—C5	1.404 (7)
Br6—C8	1.899 (6)	C5—C6	1.394 (6)
Br7—C9	1.891 (5)	C7—C12	1.374 (8)
Br8—C10	1.895 (5)	C7—C8	1.405 (7)
Br9—C11	1.886 (6)	C8—C9	1.390 (7)
Br10—C12	1.898 (5)	C9—C10	1.404 (8)
O—C7	1.389 (6)	C10—C11	1.390 (7)
O—C6	1.406 (5)	C11—C12	1.408 (8)
C1—C6—C5	122.0 (4)	C12—C7—O	125.8 (5)
C1—C6—O	116.1 (4)	C12—C7—C8	119.8 (5)
C5—C6—O	121.9 (5)	O—C7—C8	114.1 (5)
C7—O—C6—C1	125.2 (5)	C6—O—C7—C12	−39.0 (6)
C7—O—C6—C5	−56.0 (7)	C6—O—C7—C8	146.4 (4)

All Br atoms were refined with anisotropic displacement parameters. The large positive and negative differences are located near the Br atoms. Refining the C atoms with anisotropic displacement parameters yielded some of them as slightly non-positive definite, but with no significant improvement in the residual factors. Since the thermal vibrations were rather small due to the low-temperature experiment, it was decided to use isotropic C atoms in the structure model in order to avoid non-physical displacement parameters.

Data collection: *EXPOSE* (Stoe & Cie, 1997*b*). Cell refinement: *CELL* (Stoe & Cie, 1997*c*). Data reduction: *INTEGRATE* (Stoe & Cie, 1997*d*). Program(s) used to solve structure: *SHELXS*86 (Sheldrick, 1990). Program(s) used to refine structure: *SHELXL*93 (Sheldrick, 1993). Molecular graphics: *DIAMOND* (Bergerhoff, 1996).

This work was supported by the Swedish Natural Science Research council.

Supplementary data for this paper are available from the IUCr electronic archives (Reference: KA1314). Services for accessing these data are described at the back of the journal.

References

Allen, F. H. & Kennard, O. (1993). *Chem. Des. Autom. News*, **8**, 31–37.
Baharie, E. & Pawley, G. S. (1979). *Acta Cryst.* A**35**, 233–235.
Bergerhoff, G. (1996). *DIAMOND. Visual Crystal Information System.* Gerhard-Domagk-Straße 1, 53121 Bonn, Germany.
Capon, R., Ghisalberti, E. L., Jefferies, P. R., Skelton, B. W. & White, A. H. (1981). *J. Chem. Soc. Perkin Trans.* 1, p. 2464.
Domenicano, A. & Murray-Rust, P. (1979). *Tetrahedron Lett.* **24**, 2283–2286.
Il'in, S. G., Utkina, N. K., Veselova, M. V. & Struchkov, Yu. T. (1996). *Izv. Akad. Nauk SSSR Ser. Khim.* p. 756.
Kuryla, W. C. & Papa, A. J. (1979). *Flame Retardancy of Polymeric Materials*, Vol. 5. New York: Dekker.
Örn, U., Eriksson, L., Jakobsson, E. & Bergman, Å. (1996). *Acta Chem. Scand.* pp. 802–807.
Sheldrick, G. M. (1990). *Acta Cryst.* A**46**, 467–473.
Sheldrick, G. M. (1993). *SHELXL*93. *Program for the Refinement of Crystal Structures.* University of Göttingen, Germany.
Stoe & Cie (1997*a*). *XRED. Data Reduction Program.* Version 1.09. Stoe & Cie, Darmstadt, Germany.
Stoe & Cie (1997*b*). *EXPOSE. Stoe IPDS Software for Data Collection.* Version 2.87. Stoe & Cie, Darmstadt, Germany.
Stoe & Cie (1997*c*). *CELL. Program for Cell Refinement.* Version 2.87. Stoe & Cie, Darmstadt, Germany.
Stoe & Cie (1997*d*). *INTEGRATE. Program for Reduction of IPDS Data.* Version 2.87. Stoe & Cie, Darmstadt, Germany.

Acta Cryst. (1999). C**55**, 2171–2177

L-Alanyl-L-phenylalanine–2-propanol (1/2) (α-form), L-valyl-L-phenylalanine–2-propanol (1/1) and L-leucyl-L-phenylalanine–2-propanol (1/1) (β-form)

CARL HENRIK GÖRBITZ

Department of Chemistry, University of Oslo, PO Box 1033 Blindern, N-0315 Oslo, Norway. E-mail: c.h.gorbitz@kjemi.uio.no

(Received 10 June 1999; accepted 6 September 1999)

Abstract

Small crystals of L-Ala-L-Phe–2-propanol (1/2), $C_{12}H_{16}N_2O_3\cdot 2C_3H_8O$, L-Val-L-Phe–2-propanol (1/1), $C_{14}H_{20}N_2O_3\cdot C_3H_8O$, and L-Leu-L-Phe–2-propanol (1/1), $C_{15}H_{22}N_2O_3\cdot C_3H_8O$, were obtained after considerable effort. The three structures have intricate packing interactions with up to four peptide molecules in the asymmetric unit and variable hydrogen-bond connectivities for the carboxylate groups. For each peptide, two or more different crystal forms were obtained in the crystallization experiments.

Comment

For dipeptides with two hydrophobic residues our previous (Görbitz, 1997, and references therein) and ongoing work has identified two different modes of

packing and hydrogen bonding: (i) formation of hydrophobic columns in hexagonal space groups with a ~10 Å *c* axis and (ii) formation of hydrophobic layers in monoclinic or orthorhombic space groups. Usually, these crystals include cocrystallized organic solvent molecules.

L-Leu-L-Val forms layered 1/1 solvates with methanol (LVm), ethanol (LVe) and 2-propanol (LV2p) (Görbitz & Torgersen, 1999). The hydrogen-bonding patterns are very similar in these structures, and in LVe and LV2p there are special hydrogen-bonded chains involving two independent carboxylate groups with different hydrogen-bond connectivities. A modification of this pattern is also found for L-Leu-L-Leu–2-methyl-1-propanol solvate (LLmp) (Görbitz, 1999). In the current paper, three new structures of hydrophobic dipeptides, L-Ala-L-Phe–2-propanol (1/2) (AF2p), L-Val-L-Phe–2-propanol (1/1) (VF2p) and L-Leu-L-Phe–2-propanol (1/1) (LF2p) are presented. These provide additional insight into the mechanism of molecular packing and hydrogen bonding in this group of compounds.

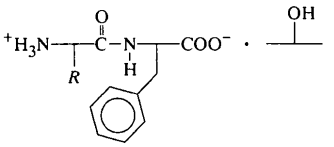

AF2p: *R* = Me

VF2p: *R* =

LF2p: *R* =

The asymmetric units of the three title solvates are shown in Fig. 1, while the crystal packing is shown in Fig. 2. All three structures are divided into hydrophilic layers with peptide main chains and alcohol hydroxyl groups connected by hydrogen bonds, and hydrophobic layers including peptide side chains and alcohol alkyl groups.

The crystal structure of AF2p is closely related to the structures of LVm, LVe and LV2p (Görbitz & Torgersen, 1999). The molecular conformations of the peptide main chains are quite similar, except for ψ_T (N2*A*—C4*A*—C12*A*—O2*A* for AF2p) which is in the range −92 to −54° for the other three structures, but −19.5 (5)° in AF2p (Table 1). The L-Phe side chain of AF2p has the common *gauche*$^-$ orientation.

In VF2p, there is pseudotranslational symmetry along the *a* axis relating *A* to *B* and *C* to *D* (Fig. 2), with a 30° rotation of the terminal-C carboxylate group as the most obvious difference between otherwise very similar geometries. The best fit superposition of structures gives a heavy-atom r.m.s. deviation of 0.262 for *A*–*B* and 0.248 Å for *C*–*D*. All four peptide molecules in the asymmetric unit are present in each hydrophilic

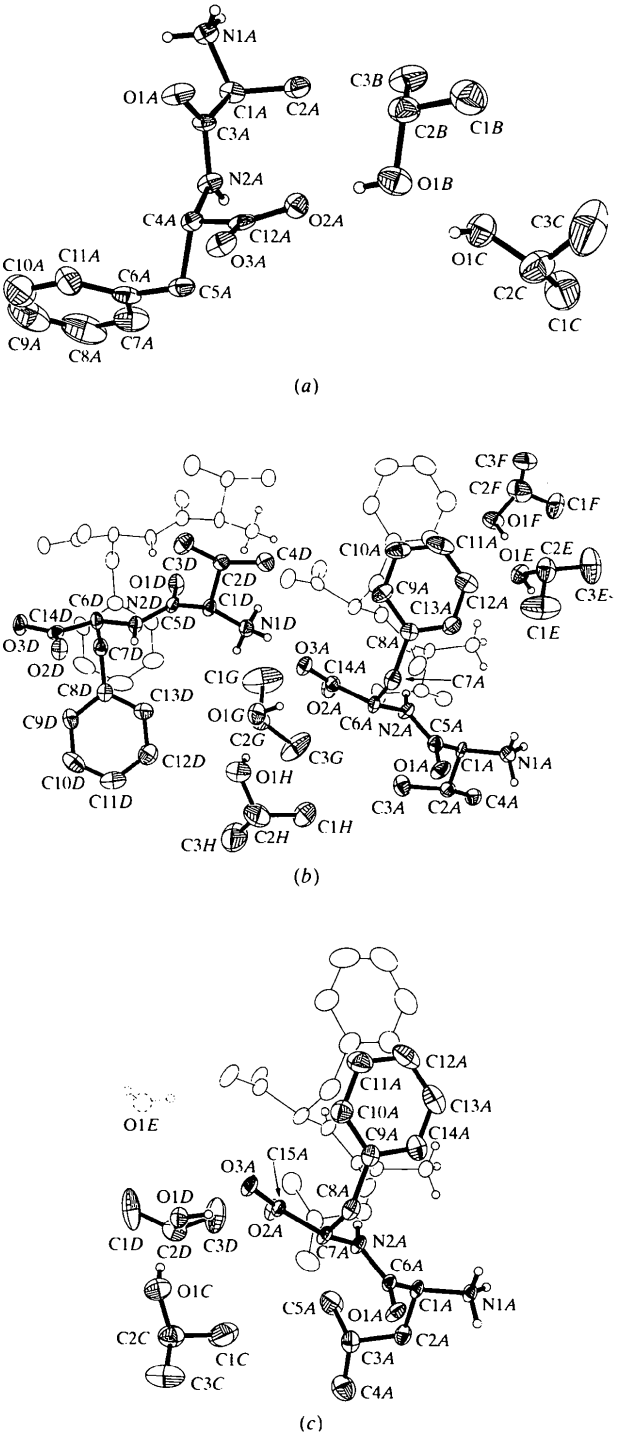

Fig. 1. The asymmetric unit of the 2-propanol solvates of (*a*) L-Ala-L-Phe (AF2p), (*b*) L-Val-L-Phe (VF2p) and (*c*) L-Leu-L-Phe (LF2p). Displacement ellipsoids are shown at the 50% probability level and selected H atoms are shown as spheres of arbitrary size. The partially occupied water molecule in the LF2p structure is shown dotted. To alleviate problems associated with the unavoidable molecular overlap, peptide molecule *B* behind *A* (VF2p and LF2p) and molecule *C* behind *D* (VF2p) are shown in a different drawing style without atomic numbering.

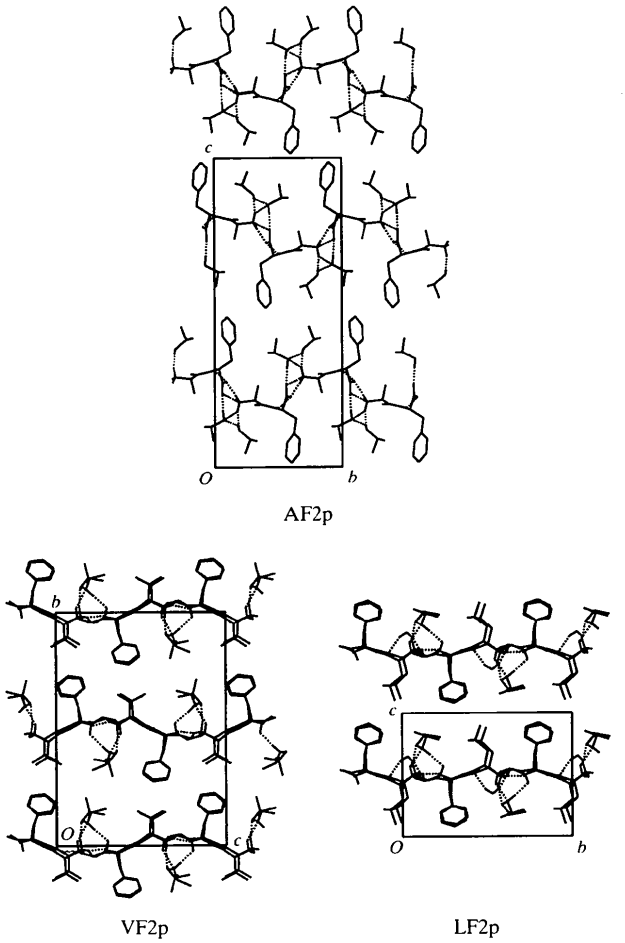

Fig. 2. The unit cell and crystal packing for the three title compounds. H atoms bonded to C atoms have been omitted for clarity. Horizontal hydrophilic layers and hydrophobic layers are seen edge-on.

layer, and neighbouring hydrophilic layers are related by the crystallographic screw axis. Additionally, a non-crystallographic screw axis parallel to the *c* axis at $x = \frac{3}{8}$ and $y = 0$ very accurately relates *A* to *C* and *B* to *D* (r.m.s. deviations 0.039 and 0.062 Å, respectively) and solvent molecules *E* to *G* and *F* to *H*. A comprehensive discussion of the symmetry and systematic absences (see below) for this special monoclinic system is given by Görbitz & Torgersen (1999) for the isomorphous and completely analogous structure of LVe.

Pseudotranslational symmetry along the *a* axis is also observed for LF2p, with a heavy-atom r.m.s. deviation of 0.218 Å for the best fit between the two molecular geometries. The peptide conformations are very similar to those observed in VF2p, as is evident from Fig. 1, with large values for ψ_T (150–159°) and a *gauche*$^+$ orientation for the L-Phe side chain. As for VF2p, neighbouring solvent molecules along the *a* axis have somewhat different orientations (Fig. 1*c*). Furthermore, it can be seen from Fig. 1 that the solvent molecules have roughly equivalent positions (albeit different orientations) in both structures. The exception is the partially occupied [0.102 (5)] solvent water molecule, which is present in LF2p only. It sits in a small cavity that is created when the L-Phe side chain is reoriented to compensate for the lack of side-chain branching at C^β for residue 1 as Val (VF2p) is replaced by Leu (LF2p).

The hydrogen-bond patterns of AF2p and LF2p (Fig. 3) are typical for hydrophobic dipeptides, in that each amino group donates two H atoms to carboxylate groups, forming head-to-tail chains, while the third amino-H atom is donated to the hydroxyl group of a cocrystallized alcohol molecule. Thus, the solvent molecules are not only included to fill cavities in the hydrophobic layers, but are indispensable parts of the hydrogen-bonding network in these structures. The AF2p pattern is identical to the pattern observed in the structure of LVm (Görbitz & Torgersen, 1999) if the 2-propanol molecule *B* is removed and the hydroxyl group of the 2-propanol molecule *C* is rotated to form an interaction with the peptide carbonyl oxygen O1*A*. Such a pattern is also observed in L-Leu-L-Tyr (LY; Krause *et al.*, 1993), in which the hydroxyl group comes from the Tyr side chain and not from a cocrystallized alcohol molecule. The three structures share the short *a* axis [AF2p 5.4825 (4), LVm 5.2890 (1) and LY 5.644 (1) Å] while, as for several other layered dipeptides, a second axis (*b* for all) is close to 12 Å, which follows from the orientation of the peptide main chain. The difference between the 11.4872 (1) Å *c* axis for LVm and the 29.4245 (19) Å *c* axis for AF2p reflects not only a doubling upon transition from space group $P2_1$ to $P2_12_12_1$, but also a further increase due to the large Phe side chain in AF2p. The larger separation between hydrophilic layers in AF2p means that the cavity filled by the methanol molecule in LVm becomes larger, and is instead filled by the 2-propanol molecule *C*. The second solvent molecule in AF2p (*B*) fills the void that

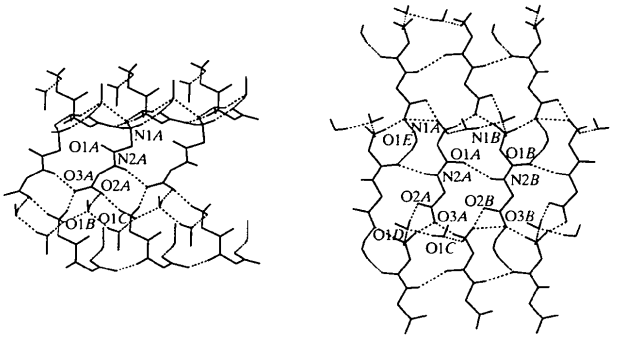

Fig. 3. The hydrogen-bonding pattern (dashed lines) in the crystal structures of AF2p and LF2p. All peptide side chains and H^α atoms have been removed for clarity; for the alcohol molecules, only C—O—H remains. Essential atom labels have been indicated. Hydrogen bonds involving LF2p water molecules with low occupancy are shown as dotted lines.

is generated when Leu in the LVm structure is replaced by Ala.

The hydrogen-bond patterns of VF2p and LF2p (Fig. 3) are almost identical, except for interactions involving the partially occupied LF2p solvent water molecule. The lengths of the *a* axes are 9.8958 (2) Å for VF2p and 10.0858 (2) Å for LF2p, which are close to the lengths of the corresponding axes for LVe and LLmp [11.0112 (1) and 10.3179 (1) Å, respectively; Görbitz, 1999]. The doubling of the *a*-axis lengths compared with AF2p and LVm results from a shift in the basic hydrogen-bond connectivity for every second carboxylate group (see Scheme below).

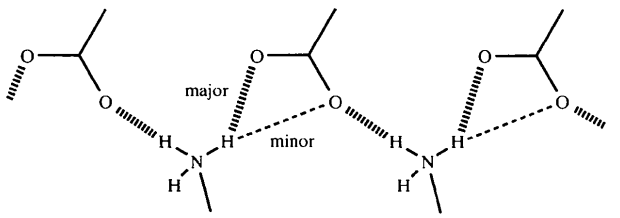

pattern I

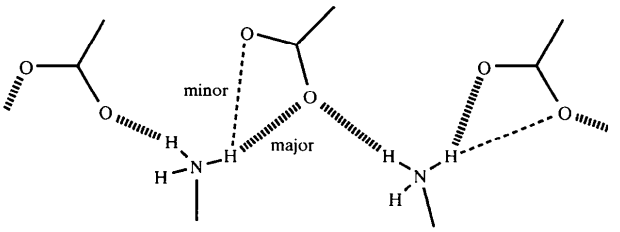

pattern II

The major components in both types of asymmetric carboxylate interactions have H···O distances in the range 1.82–1.88 Å, while H···O distances for the long minor components are in the range 2.56–2.64 Å.

An important difference between the two hydrogen-bond patterns shown in Fig. 3 is that AF2p (and thus also LVm, LVe and LV2p) has a characteristic >N—H···O interaction between the peptide group and the terminal-C carboxylate group. The carbonyl O atom, on the other hand, is not an H-atom acceptor and the C=O bond distance is short [1.201 (5) Å]. In contrast, the amide-H atoms in VF2p and LF2p are involved in alternating weak/very weak hydrogen bonds to peptide carbonyl groups, with additional weak/very weak C^{α}—H···O=C interactions varying in the opposite sequence (Tables 4 and 6). An inherently high stability for carboxylate pattern II is suggested by the fact that it can be integrated into both of these hydrogen-bond patterns, as observed in the structures of LVe and LV2p, and VF2p and LF2p, respectively.

As described in the *Experimental* section below, two or more different types of crystals were obtained in the crystallization experiments for all three dipeptides studied. The structure of the LF2p β-form (plate-shaped crystals) presented here is, judged by the cell dimensions, very closely related to the structure of the α-form [needle-shaped crystals: a = 9.9552 (3), b = 16.3894 (5), c = 23.7291 (2) Å, and β = 90.0396 (16)°]. The situation is more complicated for the relationship between the two crystal forms of AF2p for which data have been recorded. The cell volume for the AF2p β-form [a = 12.3485 (1), b = 13.5161 (1) and c = 28.9248 (4) Å] is 4828 Å^3, or 2.42 times the cell volume of the α-form. This means that the asymmetric unit of β-AF2p either contains more than two solvent molecules or possibly two independent peptide molecules. The latter alternative gives a calculated density of 1.301 Mg m^{-3}, which is high for hydrophobic dipeptides. This would leave no room for additional 2-propanol molecules, and probably not even solvent water molecules. Accordingly, such a structure would deviate from other known structures of hydrophobic dipeptides. We attempted to measure the crystal density experimentally by flotation, but no reliable results were obtained since only a limited number of very small crystal specimens was available. Attempts to solve this structure will continue.

Experimental

The title compounds were purchased from Sigma and used as received. About 0.1–0.3 mg of each peptide was dissolved in 30 µl water with subsequent vapour diffusion of 2-propanol (or other alcohol) into the aqueous solution at room temperature. The crystallizations for L-Ala-L-Phe uniformly produced very thin needles unsuitable for diffraction purposes. One test tube from these experiments was accidentally left in the laboratory and was, upon checking four months later, found to contain small blocks. Several crystals were tested and found to belong to two different forms, *i.e* an orthorhombic α form and a β form of unknown crystal system with roughly twice the unit-cell volume. The crystallization experiment was repeated, but this time only a few blocks were obtained, all of the β-modification. Additionally, some rod-like needles were formed which appear to be distinct from the other crystals. We were not able to collect data on any of these rods. The experiments and the results for L-Val-L-Phe are very similar to those for L-Ala-L-Phe. After four months, the initial very thin needles had been converted to plate-shaped crystals. Alas, the crystals proved to be very unstable and decayed instantly when exposed to air. One small single crystal, however, remained stable suggesting it was of a different modification. Data were collected from this specimen. The crystallization was repeated under the same conditions and after a period of months, small crystals had again appeared. This time all the crystals were of the stable modification, but were not larger or better than that obtained earlier. Like L-Ala-L-Phe and L-Val-L-Phe, L-Leu-L-Phe at first yielded only very thin needles (α-form) in the crystallizations. After numerous attempts, a needle just large enough for data collection was obtained.

Further experiments revealed that a second crystal form (β-form) could be obtained with low initial peptide concentration, *i.e.* 0.08 mg in 30 µl water (concentrations below 0.06 mg in 30 µl did not produce and precipitate). In the first series of crystallizations, only 2-propanol was used as precipitating agent. Later, similar experiments were carried out with seven other alcohols. Generally, very thin needles were obtained for all three peptides. The exceptions were ethanol batches of L-Ala-L-Phe and L-Val-L-Phe, which also yielded some extremely thin plates. Attempts to collect data on these crystals were unsuccessful.

Compound AF2p

Crystal data

$C_{12}H_{16}N_2O_3 \cdot 2C_3H_8O$
M_r = 356.46
Orthorhombic
$P2_12_12_1$
a = 5.4835 (4) Å
b = 12.3418 (8) Å
c = 29.4245 (19) Å
V = 1991.3 (2) Å^3
Z = 4
D_x = 1.189 Mg m^{-3}
D_m not measured

Mo $K\alpha$ radiation
λ = 0.71073 Å
Cell parameters from 4425 reflections
θ = 2–25°
μ = 0.086 mm^{-1}
T = 150 (2) K
Block
0.22 × 0.06 × 0.03 mm
Colourless

Data collection

Siemens SMART CCD diffractometer
Sets of exposures each taken over 0.2° ω rotation scans
Absorption correction: empirical (*SADABS*; Sheldrick, 1996)
T_{min} = 0.981, T_{max} = 0.997
10 243 measured reflections
3490 independent reflections

2524 reflections with $I > 2\sigma(I)$
R_{int} = 0.072
θ_{max} = 25.03°
$h = -6 \rightarrow 6$
$k = -14 \rightarrow 14$
$l = -35 \rightarrow 30$
Intensity decay: none

Refinement

Refinement on F^2
$R[F^2 > 2\sigma(F^2)]$ = 0.076
$wR(F^2)$ = 0.203
S = 1.096
3490 reflections
234 parameters
H atoms constrained
$w = 1/[\sigma^2(F_o^2) + (0.0959P)^2 + 1.2701P]$ where $P = (F_o^2 + 2F_c^2)/3$

$(\Delta/\sigma)_{max}$ = 0.021
$\Delta\rho_{max}$ = 0.34 e Å^{-3}
$\Delta\rho_{min}$ = −0.31 e Å^{-3}
Extinction correction: none
Scattering factors from *International Tables for Crystallography* (Vol. C)

Table 1. *Selected geometric parameters (Å, °) for AF2p*

O1A—C3A	1.201 (5)	N1A—C1A	1.484 (6)
O2A—C12A	1.231 (5)	N2A—C3A	1.363 (5)
O3A—C12A	1.275 (5)		
N1A—C1A—C3A—N2A	159.8 (4)		
C1A—C3A—N2A—C4A	171.4 (4)		
C3A—N2A—C4A—C12A	−77.6 (5)		
N2A—C4A—C12A—O2A	−19.5 (5)		
N2A—C4A—C12A—O3A	162.6 (4)		
N2A—C4A—C5A—C6A	−72.2 (5)		
C4A—C5A—C6A—C7A	127.6 (5)		

Table 2. *Hydrogen-bonding geometry (Å, °) for AF2p*

D—H···A	D—H	H···A	D···A	D—H···A
N1A—H1A···O1C^{i}	0.91	2.26	2.874 (5)	124
N1A—H1A···O1B^{ii}	0.91	2.37	3.030 (5)	130
N1A—H2A···O2A^{i}	0.91	1.98	2.864 (5)	162
N1A—H3A···O3A^{ii}	0.91	1.88	2.761 (5)	161
N2A—H4A···O3A^{iii}	0.88	2.17	2.945 (4)	146
O1B—H1B···O2A	0.85	1.94	2.765 (4)	166
O1C—H1C···O1B	0.85	2.12	2.857 (5)	147

Symmetry codes: (i) $1-x, \frac{1}{2}+y, \frac{3}{2}-z$; (ii) $-x, \frac{1}{2}+y, \frac{3}{2}-z$; (iii) $1+x, y, z$.

Compound VF2p

Crystal data

$C_{14}H_{20}N_2O_3 \cdot C_3H_8O$
M_r = 324.41
Monoclinic
$P2_1$
a = 9.8958 (2) Å
b = 22.3517 (6) Å
c = 16.4571 (3) Å
β = 90.023 (1)°
V = 3640.11 (14) Å^3
Z = 8
D_x = 1.184 Mg m^{-3}
D_m not measured

Mo $K\alpha$ radiation
λ = 0.71069 Å
Cell parameters from 7050 reflections
θ = 2–25°
μ = 0.084 mm^{-1}
T = 150 (2) K
Plate
0.25 × 0.10 × 0.04 mm
Colourless

Data collection

Siemens SMART CCD diffractometer
Sets of exposures each taken over 0.3° ω rotation scans
Absorption correction: empirical (*SADABS*; Sheldrick, 1996)
T_{min} = 0.979, T_{max} = 0.997
28 008 measured reflections
12 717 independent reflections

7172 reflections with $I > 2\sigma(I)$
R_{int} = 0.102
θ_{max} = 25.03°
$h = -11 \rightarrow 11$
$k = -26 \rightarrow 26$
$l = -19 \rightarrow 19$
Intensity decay: none

Refinement

Refinement on F^2
$R[F^2 > 2\sigma(F^2)]$ = 0.080
$wR(F^2)$ = 0.139
S = 1.018
12 717 reflections
683 parameters
H atoms constrained
$w = 1/[\sigma^2(F_o^2) + (0.0235P)^2]$ where $P = (F_o^2 + 2F_c^2)/3$
$(\Delta/\sigma)_{max}$ = 0.003

$\Delta\rho_{max}$ = 0.29 e Å^{-3}
$\Delta\rho_{min}$ = −0.30 e Å^{-3}
Extinction correction: *SHELXL*97 (Sheldrick, 1997*a*)
Extinction coefficient: 0.0033 (3)
Scattering factors from *International Tables for Crystallography* (Vol. C)

Table 3. *Selected geometric parameters (Å, °) for VF2p*

O1A—C5A	1.255 (4)	O1B—C5B	1.236 (4)
O2A—C14A	1.262 (5)	O2B—C14B	1.245 (5)
O3A—C14A	1.260 (4)	O3B—C14B	1.265 (5)
N1A—C1A	1.507 (4)	N1B—C1B	1.510 (4)
N2A—C5A	1.327 (5)	N2B—C5B	1.350 (5)
N1A—C1A—C5A—N2A	132.3 (5)		
C1A—C5A—N2A—C6A	172.9 (4)		
C5A—N2A—C6A—C14A	−150.8 (5)		
N2A—C6A—C14A—O2A	20.0 (7)		
C7A—C6A—C14A—O3A	−35.3 (7)		
N1A—C1A—C2A—C3A	178.0 (4)		

N1*A*—C1*A*—C2*A*—C4*A*	−58.3 (5)
N2*A*—C6*A*—C7*A*—C8*A*	61.1 (5)
C6*A*—C7*A*—C8*A*—C9*A*	98.2 (7)
N1*B*—C1*B*—C5*B*—N2*B*	121.9 (5)
C1*B*—C5*B*—N2*B*—C6*B*	172.5 (4)
C5*B*—N2*B*—C6*B*—C14*B*	−159.9 (6)
N2*B*—C6*B*—C14*B*—O2*B*	−11.7 (7)
N2*B*—C6*B*—C14*B*—O3*B*	171.8 (6)
N1*B*—C1*B*—C2*B*—C3*B*	−175.6 (5)
N1*B*—C1*B*—C2*B*—C4*B*	−53.0 (6)
N2*B*—C6*B*—C7*B*—C8*B*	61.1 (5)
C6*B*—C7*B*—C8*B*—C9*B*	94.2 (7)
N1*C*—C1*C*—C5*C*—N2*C*	130.9 (5)
C6*C*—N2*C*—C5*C*—C1*C*	173.9 (4)
C5*C*—N2*C*—C6*C*—C14*C*	−149.5 (5)
N2*C*—C6*C*—C14*C*—O2*C*	19.5 (6)
N2*C*—C6*C*—C14*C*—O3*C*	−165.7 (5)
N1*C*—C1*C*—C2*C*—C3*C*	179.3 (4)
N1*C*—C1*C*—C2*C*—C4*C*	−57.0 (5)
N2*C*—C6*C*—C7*C*—C8*C*	62.1 (5)
C6*C*—C7*C*—C8*C*—C9*C*	96.4 (7)
N1*D*—C1*D*—C5*D*—N2*D*	122.3 (5)
C6*D*—N2*D*—C5*D*—C1*D*	172.9 (4)
C5*D*—N2*D*—C6*D*—C14*D*	−159.3 (6)
N2*D*—C6*D*—C14*D*—O2*D*	−8.9 (7)
N2*D*—C6*D*—C14*D*—O3*D*	171.5 (6)
N1*D*—C1*D*—C2*D*—C3*D*	−172.1 (5)
N1*D*—C1*D*—C2*D*—C4*D*	−49.5 (6)
N2*D*—C6*D*—C7*D*—C8*D*	61.8 (5)
C6*D*—C7*D*—C8*D*—C9*D*	91.1 (7)

Data collection

Siemens SMART CCD diffractometer	9829 reflections with $I > 2\sigma(I)$
Sets of exposures each taken over 0.6° ω rotation scans	$R_{int} = 0.075$
Absorption correction: empirical (*SADABS*; Sheldrick, 1996)	$\theta_{max} = 37.78°$
$T_{min} = 0.964$, $T_{max} = 0.996$	$h = -17 \rightarrow 17$
28 092 measured reflections	$k = -27 \rightarrow 26$
17 153 independent reflections	$l = -17 \rightarrow 20$
	Intensity decay: none

Refinement

Refinement on F^2	$(\Delta/\sigma)_{max} = 0.014$
$R[F^2 > 2\sigma(F^2)] = 0.079$	$\Delta\rho_{max} = 0.41$ e Å^{-3}
$wR(F^2) = 0.169$	$\Delta\rho_{min} = -0.27$ e Å^{-3}
$S = 1.050$	Extinction correction: none
17 153 reflections	Scattering factors from *International Tables for Crystallography* (Vol. C)
447 parameters	
H atoms constrained	
$w = 1/[\sigma^2(F_o^2) + (0.0381P)^2 + 0.5370P]$ where $P = (F_o^2 + 2F_c^2)/3$	

Table 4. *Hydrogen-bonding geometry (Å, °) for VF2p, molecules A, B, E and F*

D—H···*A*	*D*—H	H···*A*	*D*···*A*	*D*—H···*A*
N1*A*—H1*A*···O2*D*^{i}	0.91	1.84	2.713 (6)	159
N1*A*—H2*A*···O3*C*^{ii}	0.91	1.94	2.786 (7)	154
N1*A*—H3*A*···O1*F*^{iii}	0.91	1.97	2.837 (7)	160
N2*A*—H4*A*···O2*A*	0.88	2.44	2.646 (4)	94
N2*A*—H4*A*···O1*B*	0.88	2.25	3.101 (5)	163
C1*A*—H5*A*···O1*B*	1.00	2.44	3.358 (6)	152
C6*A*—H6*A*···O2*B*^{iii}	1.00	2.40	3.233 (6)	141
N1*B*—H1*B*···O3*C*^{i}	0.91	1.87	2.765 (6)	167
N1*B*—H2*B*···O3*D*^{i}	0.91	1.84	2.733 (6)	167
N1*B*—H3*B*···O1*E*	0.91	2.19	2.965 (7)	143
N2*B*—H4*B*···O2*B*	0.88	2.29	2.653 (4)	104
N2*B*—H4*B*···O1*A*^{iv}	0.88	2.49	3.276 (5)	150
C1*B*—H5*B*···O1*A*^{iv}	1.00	2.23	3.171 (6)	156
C6*B*—H6*B*···O2*A*	1.00	2.30	3.256 (7)	160
O1*E*—H1*E*···O2*C*^{i}	0.84	1.84	2.675 (6)	172
O1*F*—H1*F*···O1*E*	0.84	2.07	2.896 (7)	168

Symmetry codes: (i) $x, y, z - 1$; (ii) $1 + x, y, z - 1$; (iii) $1 + x, y, z$; (iv) $x - 1, y, z$.

Compound LF2p

Crystal data

$C_{15}H_{22}N_2O_3 \cdot C_3H_8O$	Mo $K\alpha$ radiation
$M_r = 338.44$	$\lambda = 0.71073$ Å
Monoclinic	Cell parameters from 8192 reflections
$P2_1$	$\theta = 2$–$35°$
$a = 10.0858$ (2) Å	$\mu = 0.081$ mm^{-1}
$b = 16.3754$ (2) Å	$T = 150$ (2) K
$c = 11.7987$ (2) Å	Plate
$\beta = 91.698$ (1)°	0.45 × 0.35 × 0.05 mm
$V = 1947.81$ (6) Å^3	Colourless
$Z = 4$	
$D_x = 1.154$ Mg m^{-3}	
D_m not measured	

Table 5. *Selected geometric parameters (Å, °) for LF2p*

O1*A*—C6*A*	1.235 (2)	O1*B*—C6*B*	1.236 (2)
O2*A*—C15*A*	1.243 (2)	O2*B*—C15*B*	1.251 (2)
O3*A*—C15*A*	1.274 (2)	O3*B*—C15*B*	1.260 (2)
N1*A*—C1*A*	1.498 (2)	N1*B*—C1*B*	1.495 (3)
N2*A*—C6*A*	1.337 (2)	N2*B*—C6*B*	1.341 (2)

N1*A*—C1*A*—C6*A*—N2*A*	127.86 (18)
C1*A*—C6*A*—N2*A*—C7*A*	175.34 (17)
C6*A*—N2*A*—C7*A*—C15*A*	−152.55 (18)
N2*A*—C7*A*—C15*A*—O2*A*	17.5 (2)
N2*A*—C7*A*—C15*A*—O3*A*	−164.40 (16)
N1*A*—C1*A*—C2*A*—C3*A*	172.01 (17)
C1*A*—C2*A*—C3*A*—C4*A*	−178.0 (2)
C1*A*—C2*A*—C3*A*—C5*A*	59.0 (3)
N2*A*—C7*A*—C8*A*—C9*A*	65.8 (2)
C7*A*—C8*A*—C9*A*—C10*A*	98.3 (2)
N1*B*—C1*B*—C6*B*—N2*B*	124.93 (18)
C1*B*—C6*B*—N2*B*—C7*B*	176.04 (18)
C6*B*—N2*B*—C7*B*—C15*B*	−158.97 (18)
N2*B*—C7*B*—C15*B*—O2*B*	−5.9 (3)
N2*B*—C7*B*—C15*B*—O3*B*	175.00 (19)
N1*B*—C1*B*—C2*B*—C3*B*	174.51 (16)
C1*B*—C2*B*—C3*B*—C4*B*	177.79 (18)
C1*B*—C2*B*—C3*B*—C5*B*	54.6 (3)
N2*B*—C7*B*—C8*B*—C9*B*	62.1 (2)
C7*B*—C8*B*—C9*B*—C10*B*	96.6 (3)

Table 6. *Hydrogen-bonding geometry (Å, °) for LF2p*

D—H···*A*	*D*—H	H···*A*	*D*···*A*	*D*—H···*A*
N1*A*—H1*A*···O2*B*^{i}	0.91	1.81	2.715 (2)	170
N1*A*—H2*A*···O3*A*^{ii}	0.91	1.90	2.791 (2)	166
N1*A*—H3*A*···O1*C*^{ii}	0.91	2.15	2.899 (3)	140
N2*A*—H4*A*···O2*A*	0.88	2.42	2.647 (2)	95
N2*A*—H4*A*···O1*B*	0.88	2.29	3.151 (2)	168
C1*A*—H5*A*···O1*B*	1.00	2.58	3.497 (2)	153
C7*A*—H6*A*···O2*B*^{iii}	1.00	2.48	3.323 (2)	141
N1*B*—H1*B*···O3*A*^{i}	0.91	1.83	2.719 (2)	165
N1*B*—H2*B*···O3*B*^{i}	0.91	1.82	2.722 (2)	172
N1*B*—H3*B*···O1*D*^{i}	0.91	2.17	2.854 (2)	131
N2*B*—H4*B*···O2*B*	0.88	2.26	2.619 (2)	105
N2*B*—H4*B*···O1*A*^{iv}	0.88	2.57	3.372 (2)	152
C1*B*—H5*B*···O1*A*^{iv}	1.00	2.20	3.180 (2)	165

C7*B*—H6*B*···O2*A*	1.00	2.32	3.288 (2)	164
O1*C*—H1*C*···O1*D*	0.85	2.07	2.895 (2)	169
O1*D*—H1*D*···O2*A*	0.85	1.87	2.700 (2)	172
O1*E*—H1*E*···O3*B*	0.85	2.10	2.911 (12)	159
O1*E*—H2*E*···O1*B*^{v}	0.85	2.13	2.933 (10)	159

Symmetry codes: (i) $1-x, \frac{1}{2}+y, 1-z$; (ii) $-x, \frac{1}{2}+y, 1-z$; (iii) $x-1, y, z$; (iv) $1+x, y, z$; (v) $1-x, y-\frac{1}{2}, 1-z$.

The structures of AF2p (α-form) and LF2p (β-form) were solved directly using *SHELXTL* (Sheldrick, 1997*b*). The cell dimensions are rather similar to those of LVe (a = 11.01, b = 23.52, c = 12.26 Å and β = 90.01°; Görbitz & Torgersen, 1999) and the unorthodox systematic absences are the same: $h00$, $h = 4n + 2$ absent; $0k0$, $k = 2n + 1$ absent; $00l$, $l = 2n + 1$ absent. The two structures proved to be isomorphous, and the structure of VF2*p* was solved in the same indirect manner as described previously for LVe (Görbitz & Torgersen, 1999). As observed for LVe (Görbitz & Torgersen, 1999), the VF2*p* crystal used for data collection was a TLQS (twin-lattice quasi-symmetry) twin (Giacovazzo *et al.*, 1992), which was effectively treated as TLS (twin-lattice symmetry) since all reflections contained intensity from both twin components. Crystal twinning for a monoclinic system emulating orthorhombic was handled by the *SHELXTL* command *TWIN* 1 0 0 0 −1 0 0 0 −1. The fractions of the two components are 0.576 (2) and 0.424 (2). Pairs of peptide molecules related by non-crystallographic screw axes were connected by tight *SAME* 0.0002 0.0004 commands, constraining equivalent bond lengths and bond angles (but not torsion angles) to be almost similar. This procedure was tested and discussed for refinement of LVe (Görbitz & Torgersen, 1999). Furthermore, U_{ii} (i = 1, 2 or 3) and U_{12} values are the same for *A* and *C*, and for *B* and *D*, while U_{13} and U_{23} values for *C* and *D* were constrained to be $-U_{13}$ and $-U_{23}$ for the corresponding atoms in *A* and *B*, respectively. Finally, milder *SAME* 0.005 0.008 restraints were used for the geometries of the four 2-propanol molecules. A loose *SAME* 0.01 0.01 restraint was also used for bond lengths and bond angles in the two 2-propanol molecules of AF2p.

For all compounds, data collection: *SMART* (Siemens, 1995); cell refinement: *SAINT* (Siemens, 1995); data reduction: *SAINT*; program(s) used to solve structures: *SHELXTL*; program(s) used to refine structures: *SHELXTL*; molecular graphics: *SHELXTL*; software used to prepare material for publication: *SHELXTL*.

The purchase of the Siemens SMART diffractometer was made possible through support from the Research Council of Norway (NFR).

Supplementary data for this paper are available from the IUCr electronic archives (Reference: OS1078). Services for accessing these data are described at the back of the journal.

References

Giacovazzo, C., Monaco, H. L., Viterbo, D., Scordari, F., Gilli, G., Zanotti, G. & Catti, M. (1992). *Fundamentals of Crystallography*, edited by C. Giacovazzo, pp. 83–87. Oxford University Press.
Görbitz, C. H. (1997). *Acta Cryst.* C**53**, 736–739.
Görbitz, C. H. (1999). *Acta Cryst.* C**55**, 670–672.
Görbitz, C. H. & Torgersen, E. (1999). *Acta Cryst.* B**55**, 104–113.
Krause, J. A., Baures, P. W. & Eggleston, D. S. (1993). *Acta Cryst.* B**49**, 123–130.
Sheldrick, G. M. (1996). *SADABS. Program for Absorption Corrections*. University of Göttingen, Germany.
Sheldrick, G. M. (1997*a*). *SHELXL97. Program for the Refinement of Crystal Structures*. University of Göttingen, Germany.
Sheldrick, G. M. (1997*b*). *SHELXTL. Structure Determination Programs*. Version 5.10. Bruker AXS Inc., Madison, Wisconsin, USA.
Siemens (1995). *SMART* and *SAINT. Area Detector Control and Integration Software*. Version 5.03. Siemens Analytical X-ray Instruments Inc., Madison, Wisconsin, USA.

Acta Cryst. (1999). C**55**, 2177–2179

4,8-Dibenzyl-2′,4′,6′-trinitrospiro[1,3-dioxa-azulenium-2,1′-cyclohexadienide]

Oleg Ya. Borbulevych,[a] Michail Yu. Antipin[a] and Lev P. Olekhnovich[b]

[a]*A. N. Nesmeyanov Institute of Organoelement Compounds of the Russian Academy of Sciences, 28 Vavilov St, Moscow 117813, Russia, and* [b]*Department of Chemistry, Postov State University, 7 Zorge St, Rostov-on-Don 344090, Russia. E-mail: oleg@xrlab.ineos.ac.ru*

(*Received 8 July 1999; accepted 29 September 1999*)

Abstract

In molecules of the title compound, $C_{27}H_{19}N_3O_8$, the nitro groups have almost equivalent geometries. Similar observations were made for some related anionic σ complexes. However, equalization of bond lengths within the conjugated system of the cyclohexadienide ring is stronger than that in other Meisenheimer complexes.

Comment

The synthetic chemistry of electron-deficient aromatics and heteroaromatics is circumscribed by the two major mechanisms of nucleophilic aromatic substitution, *i.e.* SNAr and Vicarious Nucleophilic Substitution (VNS; Artamkina *et al.*, 1982; Buncel *et al.*, 1995). These displacement reactions form the backbone of numerous important syntheses of pharmaceuticals and potential drugs and several other classes of bioactive agents. The key intermediate in both the SNAr and VNS mechanisms is a negatively charged σ complex commonly termed a Meisenheimer complex.

Dipolar spirocyclic Meisenheimer complexes with tropylium cations are a special class of such complexes and, in general, can be considered as a new class of heterocyclic compounds. In addition, these compounds are of great interest because their formation involves acylotropic rearrangements (Knyazev & Drozd, 1995; Kurbatov *et al.*, 1997).